Characterization and modelling of mechanical behavior of a FKM sleeve for aircraft application

Meriem Bouakkaz
ENSMA, 86 360 Chasseneuil-du-Poitou, France

Daphné Berthier
Zodiac Interconnect France, 37 600 Loches, France

Stéphane Méo
CERMEL, Ecole d'ingénieurs Polytechnique de l'Université de Tours 37 000 Tours, France

The research works reported here, were conducted within the framework of research carried for a PhD thesis. The aim of this thesis is to develop the formulation of a new fluoroelastomer (FKM), for electrical wiring protection for next generation aircraft engines. Indeed, those future engines will be more efficient which implies higher operating temperature. The formulation of this new elastomer is based on a reference FKM in which nanoloads will be added to improve its mechanical performances and reach properties expected in the technical specifications. This new formulation is not yet completed. Hence, the study here reported consist in the characterization and modelling of the hyperelastic behavior and the analysis of a premature thermal ageing at 250°C on this reference material. This project was lead in order to develop a methodology that will be adjusted and applied to the new material. This paper reports the whole methodology applied and main results (experiment and modelling) are analyzed.

Nomenclature

ν	=	Poisson's ratio	W	=	Strain energy potential
E	=	Young modulus expressed in MPa	C_{ij}	=	Material parameters expressed in MPa
ε	=	Strain	λ_i	=	Principal stretch
σ	=	Stress expressed in MPa	I_i	=	Strain invariant
V_i	=	Initial volume	$\overline{\lambda_i}$	=	Deviatoric stretch
V_f	=	Final volume	$\overline{I_i}$	=	Deviatoric strain invariant
J	=	Total volume ratio			

I. Introduction

Fluoroelastomer are polymers composed of nearly 60% of fluorine by mass and have large elasticity properties. They are developed in the 1940s and 1950s by *E.I du Pont de Nemours & Company*. They have become materials of choice for use in aerospace and industrial equipment subjected to severe conditions. FKM is the designation of fluoroelastomers according to the American standard ASTM.[13] They are synthetic rubbers made by copolymerizing various combinations of monomers presented in Fig. 1[1]. Their repeat unit is a fluorocarbon. So, they are made up of several strong fluorine-carbon bonds.

FKM are particularly valued for their wide range of properties:[13]

- **Thermal:** they have excellent heat stability thanks to fluorine (with a use temperature from -30°C to +250°C). Its thermal resistance is the best of all elastomers.
- **Chemical:** they have wide chemical resistance and superior performance, especially in high temperature application in different media. Particularly, it resists to mineral oils, fuels, mineral acids, and water. However it has no resistance to polar solution as acetone or glycol.
- **Mechanical:** FKM have lower mechanical properties than the other rubbers but remained satisfying. These can be improved thanks to load addition.

FKM represent 5% of rubbers and are classified as specialist elastomers.[13] Rubbers generally are specific materials as they have different mechanical behaviors at room temperature. They are also temperature dependent. [6]

The main properties of rubbers are the following:

- **Linear elasticity for low strain:** a rubber has an elastic behavior for a strain range under 20%.
- **Hyperelasticity for large strain:** elastomers are characterized by a high deformability.
- **Viscoelasticity:** those materials exhibit both viscous and elastic characteristics when undergoing deformation. So deformation reversibility is not immediate. This property depends on load speed and temperature.

Figure 1. Main constitutive monomers of a FKM.

Zodiac Aerospace uses FKM to manufacture temperature-resistant sleeves for aircraft engines. Indeed, Interconnect division of Zodiac Aerospace manufactures and assembles a wide range of specialist elastomer and is expert in the design and manufacture of wiring systems for static and dynamic applications in safety-critical and harsh environments. Today, Zodiac works on an innovative FKM in collaboration with the CERMEL (Centre de Recherche pour les Matériaux ELastmères). This partnership was initiated in 2015 by a PHD thesis within the CIFRE agreement. The aim of the thesis is to develop a new FKM based on a reference gum to manufacture electrical wiring protection sleeve for new generation aircraft engines. Reference gum have good properties but need to be improved by load addition to be resistant enough for use conditions for applications in new generation aircraft engines. Their service temperature is higher than that of current engines since they are more efficient. The formulation is not completely perfected.[13, 14] In this report, the methodology set up to characterize and model the reference gum behavior is presented. The aim of this work is to validate this methodology and apply it to model new FKM behavior. The modelling long-term objective is to develop a digital tool pre-sizing for the protective sleeves which will be composed of this new FKM.This study reported here is mainly focused on hyperelastic/elastic behavior and the effect of a thermal ageing on the fluoroelastomer properties. Only thermal ageing at 250°C is analyzed.

II. Method and tools

The methodology established to characterize this reference gum has been defined by the objectives of the numerical modelling. Thus, modelling choices were determined by what we want to observe on the digital model and modelling choices predetermine the different mechanical tests and experimental conditions to use. Material parameters of hyperelastic models are identified from the experimental data. Then, they are implemented on the digital model. We used Abaqus CAE[17] for modelling. The methodology set up for the study is given in Fig. 2:

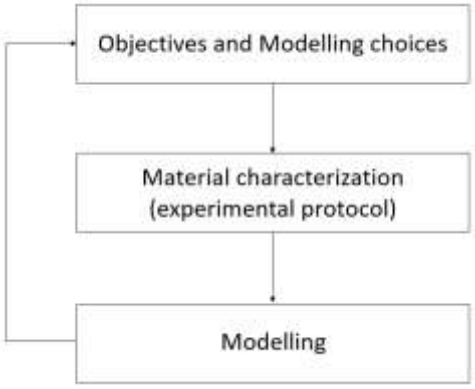

Figure 2. Methodology

A. Methodology

Firstly, the objective has been to model the sleeve behavior during its service life that is when the sleeve material has a stabilized behavior. The strain imposed by electrical wiring harnesses geometry is constant and relaxation time is reached. Thus, the material leading behavior is hyperelasticity. The approach is the following:

- **1st step: only hyperelastic behavior at room temperature is considered**

Thermo-mechanical coupling of the application is first ignored. So, the temperature effect is not considered. The second order Mooney-Rivlin model (with five parameters) is used to identify hyperelastic constitutive law of the material at room temperature. We choose this model for its performance and because it is already implemented on Abaqus CAE. We perform two types of tests to identify those five parameters: uniaxial tension test and planar tension test (pure shear).

In the case of a first order Mooney-Rivlin model (with two parameters), the parameter identification from results of uniaxial tension test gives a unique value pair which is the single solution. However this one can be physically not admissible mainly if one of the two identified parameters is negative.[9, 10] Pure shear testing allows to verify those parameters, hence it improves physical sense of the solution but it degrades the correlation between experimental results and modelling in terms of digital divide. Other tests would be necessary to ensure a better identification.[15, 16] This is even more true to identify second order Mooney-Rivlin parameters. Available means has only allowed to perform uniaxial tension test and planar tension test. So, identified parameters are not totally reliable but are sufficient to provide a suitable behavior modelling. Moreover, uniaxial tension test allow to identify elastic parameter of the material: Young modulus for stiffness evaluation and Poisson's ratio which identifies the material compressibility.

- **2nd step: temperature effect is taken into account on the hyperelastic behavior**

The same procedure has been undertaken to consider the temperature effect on the hyperelastic behavior of this FKM. Mechanical tests were performed for different times of thermal ageing. Test samples were put in an oven at a 250°C and tested at several time periods. Technical specifications of the new FKM impose a temperature endurance during at least 7 days at 260°C. More precisely, it is specified tensile strength, tear strength and elongation at break of the material must have a little evolution before and after thermal ageing (a variation <20%).[13, 14] Laboratory's available means only allowed us performing test at a maximum temperature of 250°C. For each time period, we obtained results for uniaxial tension test and planar tension test with which we identified material parameters for hyperelastic behavior in the same way than the first step. So, we considered new parameters for each thermal ageing state as if the material, for each ageing time, represented a new material. As first approximation, we considered Poisson's ratio independent of the temperature effect. So, it remains constant for each thermal ageing time period.

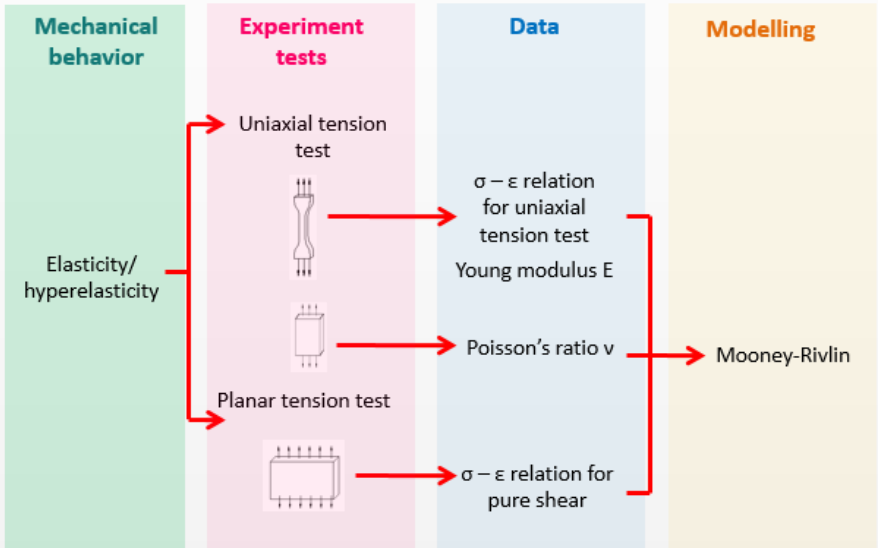

Figure 3. Hyperelastic behavior characterization

B. Mooney-Rivlin model

Hyperelastic constitutive laws are used to model materials that respond elastically when subjected to very large strains. They account both for non-linear material behavior and large shape changes. Hyperelasticity is governed by a non-linear relation binding stresses and strains. All hyperelastic models are constructed as follow. Stresses are obtained by differentiating a strain energy potential W. It defines the strain energy stored in the material per unit of reference volume (volume in the initial configuration) as a function of the strain at that point in the material. The hyperelastic behavior study needs to know a strain energy density assumed proportional to the free energy per unit of volume. The stress-strain relation is defined by specifying its strain energy density as a function of deformation gradient tensor. This ensures that the material is perfectly elastic, and also means that we only need to work with a scalar function. This strain energy density is expressed in terms of principal stretches or strain invariants.[7, 8, 15] Those are formulated as a function of principal stretches just as follow (see Eqs. (1), (2) and (3)):

$$I_1 = \lambda_1^2 + \lambda_2^2 + \lambda_3^2 \tag{1}$$

$$I_2 = \lambda_1^2\lambda_2^2 + \lambda_2^2\lambda_3^2 + \lambda_1^2\lambda_3^2 \tag{2}$$

$$I_3 = \left(\frac{V_f}{V_i}\right)^2 = \lambda_1^2\lambda_2^2\lambda_3^2 \tag{3}$$

Moreover, hyperelastic models are based on the assumption of isotropic behavior throughout the deformation history. Hence, the strain energy potential can be formulated as a function of the strain invariants. By using classical thermodynamics equations (first and second laws of thermodynamics of continuum theory) and, in the case of elastomers assumed homogeneous and isotropic, stress derives from the strain energy density.[7]

The generalized Mooney-Rivlin model is formulated as a function of strain energy as power series with the two strain invariants I_1 and I_2. This model is implemented in Abaqus as follows (see Eq. (5) [5]):

$$W_{MR_N} = \sum_{i,j=1}^{N} C_{ij}(\bar{I}_1 + 3)^i(\bar{I}_2 + 3)^j + \sum_{k=1}^{N} \frac{1}{D_k}(J-1)^{2k} \tag{4}$$

Equation (6) gives expression of second order Mooney-Rivlin strain energy potential:

$$W_{MR_2} = C_{10}(\bar{I}_1 + 3) + C_{01}(\bar{I}_2 + 3) + C_{20}(\bar{I}_1 + 3)^2 + C_{02}(\bar{I}_2 + 3)^2 + C_{11}(\bar{I}_1 + 3)(\bar{I}_2 + 3) + \frac{1}{D}(J-1) \tag{5}$$

Where W_{MR} is the strain energy per unit of reference volume; N define the order. C_{ij} and D_i are temperature-dependent material parameters ($C_{00} = C_\infty = 0$). $\bar{I}_1$ and $\bar{I}_2$ are the first and second deviatoric strain invariants defined as (see Eqs. (6) and (7)):

$$\bar{I}_1 = \bar{\lambda}_1^{\,2} + \bar{\lambda}_2^{\,2} + \bar{\lambda}_3^{\,2} \tag{6}$$

$$\bar{I}_2 = \bar{\lambda}_1^{\,(-2)} + \bar{\lambda}_2^{\,(-2)} + \bar{\lambda}_3^{\,(-2)} \tag{7}$$

$\bar{\lambda}_i = J^{-\frac{1}{3}}\lambda_i$ are the deviatoric stretches with J the Jacobian of the transformation (total volume ratio). $J = 1$ for complete incompressibility. The first term is the Mooney-Rivlin model in the case of incompressible material, the last term takes into account material incompressibility. [15]

First order Mooney-Rivlin model fits with the hyperelastic behavior of non-loaded rubber for low strains (< 100%). For loaded rubber, which is our case, this law generally gives a poor approximation of experimental results that's why we chose a second order Money-Rivlin model.[12] Hence, we use the simplest model to obtain the best correlation between modelling and experimental results.

III. Experimental study

A. Sample

Test samples are in thin film format. This format has been chosen for the thesis research works for an economic interest. Indeed, thin films allow using less material than a standard sample. The aim of the thesis is to develop a

material with specific properties based to an existing FKM which is used as reference. Nanoloads will be added into this reference gum in order to improve its mechanical properties. Those nanoloads are expensive that's why thin film format has been chosen for those test samples. They were manufactured in lab by hand coating process at temperature and pressure room. Experiment protocol to produce thin film has a significant impact on samples quality. The protocol doesn't allow the controlling of overall parameters. So it is difficult to obtain a satisfying repeatability on sample quality. We can observe variations concerning thickness, surface finish and we cannot control the presence of air-bubbles trapped into the thickness. Those three parameters affect mechanical tests. So we need to repeat test several time to obtain workable results.

With the experimental protocol, we obtained thin film with a thickness of 0.4 (+/-0.05)mm. Sleeves are manufactured in standard thickness from 2 to 7mm. Mechanical tests were performed between lab thin film format and manufactured format and results show thin film format behavior is consistent with manufactured format.[14] Three types of geometry sample were produced to complete overall tests. They are shown in Fig 3.

B. Results at room temperature

The first test campaign allowed to determine the material elastic properties by evaluating the Young modulus and the Poisson's ratio which respectively characterize the stiffness and the compressibility of the material. It has to be noted that Young modulus notion has no real sense to describe an elastomer stiffness but this is a common understanding within scientific community. The term here refers the elastic modulus which is determined with the linear area of the strain-stress curve for uniaxial tension. The values are given in table 1.

Table 1. Elastic properties of the material

Parameter	Values
ν	$0{,}44 \pm 0{,}04$
E	$5{,}0 \pm 0{,}5\ MPa$

Poisson's ratio value is lower than anticipated but is consistent. Poisson's ratio value is generally between 0.48 and 0.50 for elastomers because of their low compressibility.[6] This difference should come from the thin film manufacturing process. Indeed, samples were manufactured at room pressure so air micro-bubbles can be trapped into the thickness. Concerning the Young modulus, its value is consistent with what we had anticipated.

On the other hand, we obtained strain-stress curve for uniaxial tension and pure shear. With those experimental data we identify C_{mn} parameters of the second order Mooney-Rivlin model thanks to reverse identification module on Abaqus CAE. This module allows evaluating hyperelastic material behavior by automatically creating response curves using selected strain energy potentials.[5] Computed parameters are given in Fig. 5 and the comparison between experimental and numerical strain-stress curves for uniaxial tension and pure shear is in Fig. 4.

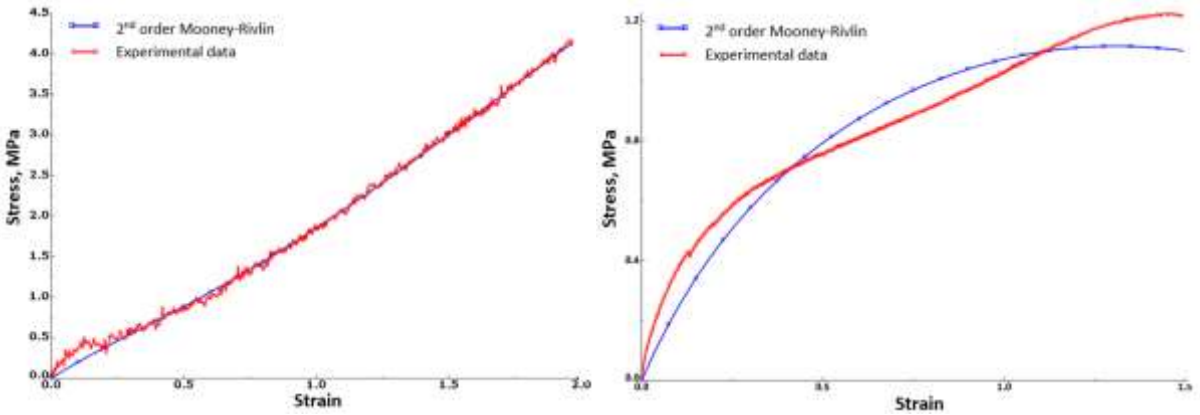

(a) (b)

Figure 4. Comparison between experimental data and 2nd order Mooney-Rivlin model *for uniaxial tension (a) and pure shear (b).*

Abaqus identification is questionable. As it can be observed, the models closely fit the experimental data. They give reasonable degree of agreements between real and computed data (more for uniaxial tension data than planar tension data). The degree of fitting for the second order Mooney-Rivlin model even though appears satisfactory from the plot, is however not recommendable for further use due to its unstable computed data as indicated from the evaluation report in Abaqus shown in Fig. 5. This implies that the use of this model will give rise to unstable results in the sense that application of a load to a material point can lead to arbitrary deformations.[3]

Mooney Rivlin model should satisfy stability criterion in order to produce real behavior of the material. Abaqus makes this check using the Drucker Stability Postulate,[5] that implies the incremental internal energy of a material can only increase. This is expressed by the following conditions (see Eq. 8):

$$\frac{\partial \sigma_{ij}}{\partial \varepsilon_{ij}} \geq 0 \text{ and } \partial \sigma_{ij} \partial \varepsilon_{ij} \geq 0 \tag{8}$$

This means that the tangential stiffness matrix must be positive definite.[3] Materials that satisfy these criteria are generally well-suited for numerical analysis, while materials that fail to satisfy this criterion are likely to present difficulties as non-uniqueness or singularity during the solution process. [8]

To be unconditionally stable, the above mentioned conditions leads certain restrictions on the Mooney-Rivlin parameters as mentioned below in equation (9): [4]

$$C_{10} + C_{01} > 0,\ C_{20} > 0,\ C_{02} > 0 \text{ and } C_{20} + C_{02} + C_{11} > 0 \tag{9}$$

It is not verified here since 3out of 5 identified parameters are negative.

```
 HYPERELASTICITY - POLYNOMIAL STRAIN ENERGY FUNCTION WITH N =   2

                  D1                C10               C01
                  D2                C20               C11               C02

             0.346124187       0.461847131      -0.113227339
              0.00000000      -5.365780776E-02   0.287799529      -0.248088224



                  STABILITY LIMIT INFORMATION


WARNING: UNSTABLE HYPERELASTIC MATERIAL


    UNIAXIAL TENSION:        UNSTABLE AT A NOMINAL STRAIN LARGER THAN        0.8400
    UNIAXIAL COMPRESSION:    UNSTABLE AT A NOMINAL STRAIN LESS THAN         -0.2818
    BIAXIAL TENSION:         UNSTABLE AT A NOMINAL STRAIN LARGER THAN        0.1800
    BIAXIAL COMPRESSION:     UNSTABLE AT A NOMINAL STRAIN LESS THAN         -0.2628
    PLANAR TENSION:          UNSTABLE AT A NOMINAL STRAIN LARGER THAN        0.3800
    PLANAR COMPRESSION:      UNSTABLE AT A NOMINAL STRAIN LESS THAN         -0.2754
    VOLUMETRIC TENSION:      STABLE FOR ALL VOLUME RATIOS
    VOLUMETRIC COMPRESSION:  STABLE FOR ALL VOLUME RATIOS
```

Figure 5. Abaqus computed parameters of 2nd order Mooney-Rivlin model andstability check

C. Results after thermal ageing

With the second experimental campaign, we obtained strain-stress curves for uniaxial tension and pure shear with different thermal ageing time conditions. The test samples were put in an oven at a temperature of 250°C. After a fixed duration, samples had been out of the oven. Then, they are maintained at room temperature during a day to consider only the thermal ageing effect on test results and not the sample temperature. Measurements were carried out for several periods mentioned in table 2. Those are been chosen arbitrarily to obtain thermal ageing effect in the short and long term.

Table 2. Thermal ageing measurement at 250°C

Time periods (days)	3	7	14	28	56	84	112	125

Figure 6 gives results before and after thermal ageing only for uniaxial traction until 56 days. After 56 days, test samples were not workable since samples broke when we removed them from oven at the 84th day.

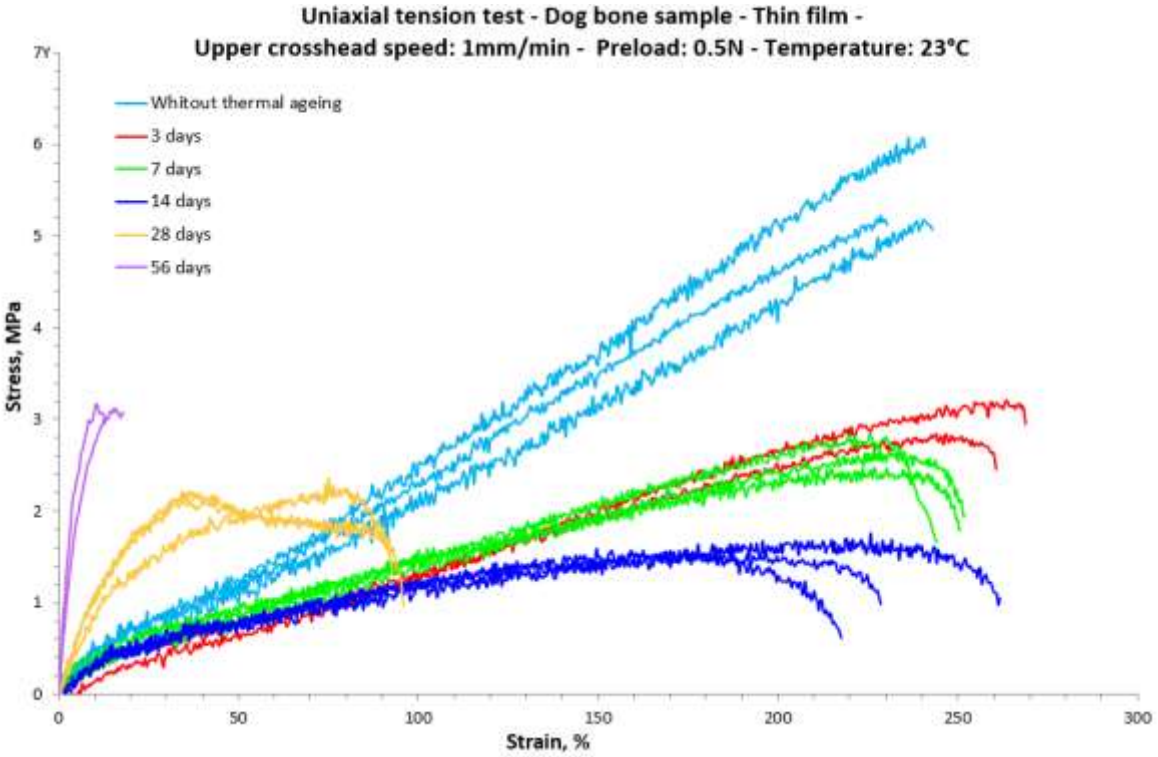

Figure 6. Uniaxial traction results without and with thermal ageing

Results analysis can be divided into three parts. First, we can observe a stress softening for samples subjected to a thermal ageing from 3 to 14 days. Their stress values are lower than samples remained at room temperature without any thermal ageing. Moreover, those samples (3, 7 and 14 days at 250°C) have a similar elongation at break and a similar stabilized behavior until ε =100 %. With those observations, we can assume that it cannot be a degradation mechanism since the elongation at break is the same for the three different periods at temperature. Otherwise, different elongation at break should have been observed. However, we can suppose it can be a kind of Mullins effect due to the energy provided by thermal loading. Indeed, Mullins effect appears as a stress softening after the first cycle of a cyclic mechanical loading. It is an irreversible phenomenon. So we supposed thermal ageing provides enough energy to create this stress softening as the same way than mechanical loading. In the purpose of verifying this hypothesis, we performed cyclic loading on aged and non-aged samples until accommodation occurs on their strain-stress curve. If strain-stress curves are similar in both cases at the accommodation, it proves that the energy provided by thermal ageing is the same nature as energy provided by mechanical load. Because of non-repeatability of results and due to a lack of sample this result does not allow a firm conclusion. However, this hypothesis seems not to be verified a priori.

After 28 days at 250°C and beyond, we can see on results a stress increase and an elongation at break decrease which is evidence of material stiffening. It is more rigid and consequently more brittle. Degradation mechanism is clearly being occurred. We validate this assumption thanks to DSC (Differential Scanning Calorimetry) and TGA (Thermo gravimetric Analysis) analyses which prove degradation mechanism occurs between 28 days and 56 days at 250°C. The question is to know if this is a thermolysis or thermo-oxidation phenomenon. Considering the low sample thickness, we can consider degradation is only due to a thermo-oxydation mechanism.

Overall test results show a premature property loss. This is contrary to expected results. Indeed, FKM are valued for their high temperature resistance and after only 3 days we can see a softening effect, and a brittle behavior appears for 28 days at 250°C. This may be attributing to the experimental conditions. A continuum temperature at 250°C is too harsh for such an application. Zodiac sleeve must be subjected to high temperature. The medium service temperature is inferior to 250C°C but with momentary peaks at 300°C. Besides, due to the small thickness degradation mechanism occurs faster. This could be verified by performing test with thickness sample of the same order of magnitude as thickness manufactured sleeve to evaluate the effect of such harsh conditions.

Conclusions for pure shear results are the same that's why they are not mentioned here.

IV. Numerical modelling

A. Hypothesis and choices of modelling approach

To simplify the modelling on Abaqus, the following hypotheses are considered for the material:

- **Isotropic:** the behavior of the material is independent of the initial orientation of the material with respect to the loading.
- **Homogeneous:** mechanical properties are the same in the whole material volume.
- **Almost incompressible:** the material is a rubber, so there is a little volume change. Elastomer can be considered as almost incompressible material. However, it is a strong hypothesis. Indeed, in cases where the material is highly confined, the compressibility must be modeled correctly to obtain accurate results. This is not the case for this application. So the degree of compressibility is typically not crucial. It would be quite satisfactory to assume that the material is fully incompressible: the volume of the material cannot change except for thermal expansion. However, considering a fully incompressibility may cause difficulties to solve the problem numerically. A low compressibility is needed to insure stability calculation.
- **Without thermal history**: the material has not been subjected to any thermal ageing and there is no thermo-mechanical coupling. Any internal heat production is assumed to be equal to zero. Consequently, self-heaiting is negligible. This last hypothesis is valid for this application because characterization tests were performed on thin sample. Hence, self-heating can't be significant for material low thickness.

B. Modelling

- **Geometry**

The aim of this numerical model is to develop a pre-sizing tool for Zodiac Aerospace sleeves. Currently, to characterize and pre-size those sleeves, it performs thermal speed variation mechanical tests. They allowed to evaluate how a tear caused by a sharp corner due to a connector or a ferrule is propagating into the sleeve during a prolonged thermal cyclic loading (see Fig. 7).

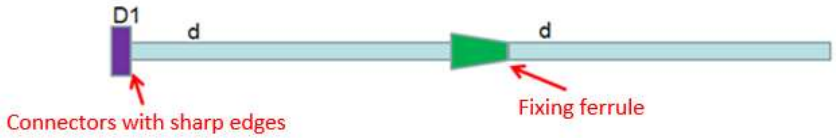

Figure 7. Schematic representation of an electrical wiring

This system is composed of a steel mandrel with a shouldered geometry (see Fig. 8). It represents the assembly electrical wiring with a connector or a ferrule. A sleeve sample is fitted on the mandrel. Its thickness is 0.7 mm. The whole assembly is subjected to a thermal cyclic loading, from -40°C to 250°C during 3000 hours.[14]

Figure 8. System for thermal speed variation mechanical tests

For the numerical modelling, we chose to reproduce the system geometry so it is modelled by a 2D axis symmetric geometric model to simplify calculation. Moreover, we modeled the steel mandrel to avoid steering the calculation with boundary conditions and avoid mathematical singularities. So we modeled the assembly system with two parts according the following way:

- Mandrel: This part is modeled by a rigid body. Indeed, mandrel stiffness is higher than sleeve stiffness so it can be considered as an infinitely stiff part face to sleeve.
- Sleeve: This part is modeled as a deformable and axisymmetric part due to its geometry.

- **Loading and boundary conditions**

For the purpose of completing and improving the numerical model in the future, it is set by four steps which integrate the sleeve swelling and its fitting on the electrical wiring. The sleeve is deformed to a maximum of 100% during the fitting process on electrical wiring. Viscoelasticity is the material leading behavior during those phases. Thanks to this modelling with several steps, material viscoelastic behavior can be added next. The expected result for our study were restricted to the sleeve behavior when it is already set up on the mandrel and it is stable (relaxation time has been already reached). Four steps are described below:

- **Step 0: Initial**
  It describes boundary conditions to the initial state system. Those conditions are the following:
  Bonded connection on mandrel: U1=U2=U3=R1=R2=R3=0
  Symmetry boundary conditions on sleeve to avoid rigid body motions: U2=U3=R1=0

- **Step 1: Sleeve expansion**
  Sleeve is swelling until it reaches 100% of deformation. Mandrel is still clamped.

- **Step 2: Mandrel displacement**
  Mandrel moves to sleeve. There is no contact between internal sleeve surface and mandrel surface because sleeve is still subjected to deformation.

- **Step 3: Sleeve fitting on mandrel**
  Sleeve is being set up on mandrel as it is no longer subjected to deformation. There is a contact between the two parts. Friction is neglected between surfaces.

We only used displacement conditions in this model. Those conditions are summed up in Fig. 9.

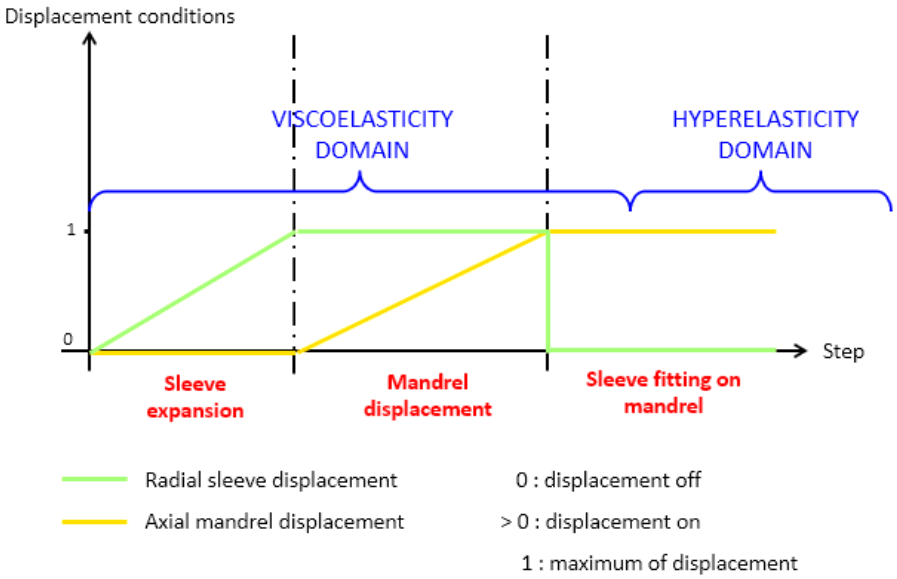

Figure 9. Schematic representation of displacement conditions

- **Material properties**

We use a hyperelastic constitutive law with a second order Mooney Rivlin model with parameters identified as explained in section II.A. without considering thermal ageing. Mooney Rivlin paramters used are those shown in Fig. 5.

- **Meshing**

Volumetric locking is exhibited by incompressible materials such as rubber having Poisson's ratio near or equal to 0.5. To offset this problem, we use hybrid finite elements. Those elements introduce extra independent variables as nodal variables during the discretization of a partial differential equation problem but they burden calculation. We used CAX8H element, which is an 8-node hybrid biquadratic axisymmetric quadrilateral element. [5] We also used a structured meshing because of geometry simplicity.

C. Results and discussion

We obtained first results with our digital model. They are given in Fig. 10. Qualitatively, they are compliant with what we expected. Sleeve behavior on the model seems to correspond to the reality notably to the mandrel shoulder area. Logarithmic strain are negative which shows sleeve model works in compression. It is physically consistent as mandrel is a rigid body. We can also notice that absolute value of logarithmic strain is higher for sleeve portion located on the mandrel portion where radius is the greatest. This is true since this in this area where pressure is the strongest. Singularities were particularly expected in this area due to non linarites of the FKM behavior. Even if the calculation converges toward a solution, this might be questionable because of our Mooney-Rivlin model quality which has a conditional stability (explained in section III.B).

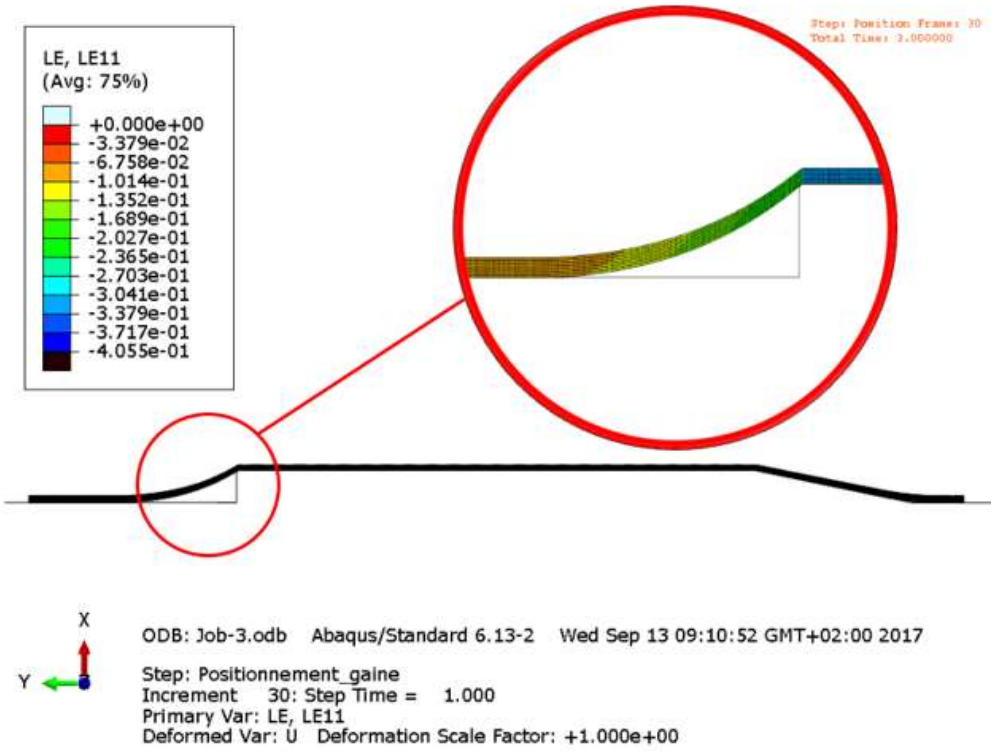

Figure 10. Abaqus results of the sleeve modelling

V. Conclusion

The methodology which was established allowed to yield significant results and some conclusions for the pursuit of work research. Those points are detailed in table 3 below:

Table 3. Discussion and recommendations

	Advantage	Disadvantage	Improvement
Experimental part	Workable and consistent results were obtained. Evaluation of a premature thermal ageing effect was obtained.	Difficulties to obtain repeatable sample quality with the protocol of thin film sample manufacturing as mentioned in section III.A	Improve experimental protocol for thermal ageing and complete additional test to verify assumptions made on preliminary results. Viscoelastic behavior characterization: some relaxation tests are performed but results weren't deeply exploited.
Modelling part	Numerical model is not steering by boundary conditions to avoid singularities or non-convergent solution. Model made by 4 steps to integrate a viscoelastic behavior model in the future.	Conditional stability of our model. No thermo-mechanical coupling.	Optimization of Mooney-Rivlin coefficients. Add a thermo-mechanical coupling by evaluating and implementing a coefficient of thermal expansion. Add a viscoelastic model.

References

Periodicals

[1]M. Biron, "Elastomères fluorocarbonés," Techniques de l'ingénieur, 2008, vol. N°2820, pp. 24.

[2]G. Palmieri, M. Sasso, G. Chiappini, and D. Amodio, "Virtual fields method on planar tension tests for hyperelastic materials characterisation," Strain, vol. 47, no. SUPPL. 2, pp. 196-209, 2011.

[3]I.J. Abubakar, P. Myler, and E. Zhou, "Constitutive Modelling of Elastomeric Seal Material under Compressive Loading". Modeling and Numerical Simulation of Material Science, 2016, 6, pp 28-40.

[4]N. Kumar V. Venkateswara Rao, "Hyperelastic Mooney-Rivlin Model: Determination and Physical Interpretation of Material Constants", MIT International Journal of Mechanical Engineering, Vol. 6, No. 1, January 2016, pp. 43-46

Books

[5]Simulia and Dassault Systèmes, Abaqus 6.12 - Analysis User's manual, 2012.

[6]G. Petitet and M. Barquins, Matériaux caoutchouteux : Morphologie, formulations, adhérence, glissance et usure. 2008.

[7]R. W. Ogden, Ellis Horwood, Series In Mathematics and its Applications, 1984.

[8]J Busfield, A Muhr, Constitutive Models for Rubber III: Proceedings of the Third European Conference on Constitutive Models for Rubber, London, UK, 15-17 September 2003

Reports, Theses, and Individual Papers

[9]S. Méo, "Modélisation numérique du comportement mécanique de structures en élastomère : de l'élasticité à la thermo-visco-hyperélasticité", Université de la Méditérranée Aix-Marseille II, 2012.

[10]A. Boukamel, "Modélisations mécaniques et numériques des matériaux et structures en élastomères," Université de la Méditérranée Aix-Marseille II, 2006.

[11]A. Delattre, "Caractérisation et modélisation du comportement hyper-viscoélastique d'un élastomère chargé pour la simulation de pièces lamifiées élastomère-métal et étude en fatigue", Université François Rabelais de Tours, 2014.

[12]A. Vandenbroucke, "Etude du comportement mécanique pour différents elastomères : caractérisations expérimentale et numérique", Université de Bretagne Sud, 2013.

[13]D. Berthier, "Rapport - Formulation, caractérisation, modélisation d'un fluoroélastomère pour application coiffe et tube haute température de protection de faisceaux," 2015 (unpublished).

[14]D. Berthier, "Rapport essais préliminaires," 2017 (unpublished).

[15]C. Nadot Martin, Cours ENSMA A3 - Grandes Déformations. 2017.

[16]S. Cantournet, "Comportement des Matériaux : Grandes Déformations," 2013.

Computer Software

[17]Abaqus CAE, Software Package, Ver. 6.12, SIMULIA, Dassault Systèmes, 2012.